# MULTI-OBJECTIVE OPTIMIZATION OF STAND-ALONE COST-EFFECTIVE RENEWABLE ENERGY SYSTEMS: THE ROLE OF STORAGE TECHNOLOGIES IN CURTAILMENT AND COST MINIMIZATION

Mattia Calabrese[1]*, Andrea Ademollo[1], Carlo Carcasci[1]

[1]University of Florence, Department of Industrial Engineering, Florence, Italy

*Corresponding Author: mattia.calabrese@unifi.it

## ABSTRACT

The urgent need to reduce global $CO_2$ emissions demands an accelerated transition to renewable energy systems. In this context, stand-alone renewable systems in remote areas are increasingly relevant, as such systems often rely on diesel generators that contribute to high $CO_2$ emissions and operating costs. This study investigates the design of a fully renewable energy system for a Mediterranean island, relying on both photovoltaic and wind energy. To achieve this, a multi-objective optimization framework is developed, targeting the minimization of the Levelized Cost of Electricity (LCOE) and renewable energy curtailment. The intermittency of renewable energy sources necessitates the use of storage systems. This study evaluates three energy storage configurations: battery storage, hydrogen storage, and a hybrid solution combining the two technologies. The hydrogen storage system includes an electrolyzer to convert excess electricity into hydrogen, a compressor and tank for storing hydrogen at the desired pressure, and a fuel cell to generate electricity when needed. The results demonstrate the shortcomings of both storage systems when employed independently. Consequently, the hybrid solution, which combines the high efficiency of batteries in short-term storage with the long-term reliability of hydrogen systems, represents the optimal selection. However, the analysis also highlights a trade-off between minimizing LCOE and renewable energy curtailment due to the high cost of storage systems. Increasing production capacity, while accepting a degree of curtailment, is currently more cost-effective. A key focus of the study is identifying threshold storage system costs at which the LCOE and curtailment cease to be conflicting objectives. This price gap serves as a critical indicator of the need for cost reductions in storage technologies to ensure economic sustainability and efficient utilization of renewable energy sources. By providing a comprehensive assessment of the interdependence between economic and technical factors across diverse storage systems, this study offers valuable insights into the design and optimization of stand-alone renewable energy systems for remote areas.

## 1 INTRODUCTION

Isolated islands, due to their limited interconnections with the national grid, continue to rely heavily on Diesel Generators (DGs) for electricity generation. For this reason, they have become focal points for transitioning to 100% Renewable Energy Systems (RESs). The shift towards RESs is primarily driven by the need to mitigate environmental impacts and reduce energy costs, which on islands can be up to ten times higher than on the mainland due to the high and volatile price of diesel (IEA, 2024). Meschede et al. (2022) noted that despite the necessity of 100% RES to meet zero greenhouse gas emission targets, research on such systems remains limited in the literature. In fact, integrating high shares of Variable Renewable Energy Sources (VRESs) such as solar and wind into these systems presents significant operational challenges, among which renewable energy curtailment is a major concern. In grid-connected systems, excess renewable energy can often be exported to neighboring grids, thereby alleviating curtailment issues. In contrast, off-grid islands must maintain a strict balance between local generation and demand, making curtailment a more pressing issue. Energy Storage Systems (ESSs) offer a potential solution by mitigating the intermittency of VREs and reducing curtailment. However, the high capital costs associated with current storage technologies often make oversizing renewable energy plants a more economically attractive alternative, even at the cost of a certain degree of curtailment. This approach leads to suboptimal utilization of renewable resources and increases the overall capital expenditure per unit of energy delivered. Additionally, in small island environments, the need to oversize renewable installation is constrained by limited land availability. Song et al. (2018) highlighted that electricity curtailment reduces the capacity factor of renewable power systems, thereby increasing their required capacity and, consequently, their land use, construction-related shipping, and maintenance costs.

Several studies analyzed the integration of storage systems in isolated locations. Brinkhaus et al. (2011) found that incorporating batteries and hydrogen storage enhances system reliability, making it particularly suitable for off-grid applications. Marocco et al. (2022) demonstrated that hydrogen storage becomes advantageous when $CO_2$ emission constraints are imposed, thereby reducing reliance on diesel generators. This paper examines three electricity storage configurations: Battery Electricity Storage System (BESS), Hydrogen Storage System (HSS), and hybrid storage (a combination of battery and hydrogen). By analyzing these configurations, the study evaluates the economic impact of storage hybridization at different levels of renewable energy curtailment.

To do this, a multi-objective optimization framework is employed, where typical objectives in the literature include system costs, such as Levelized Cost of Electricity (LCOE) (Borhanazad et al., 2014) or annual costs (Mahbub et al., 2017), and environmental aspects, particularly $CO_2$ emissions (Mahbub et al., 2016). While curtailment has also been used as an optimization objective (Wang et al., 2019), it remains less frequently addressed. In this study, the optimization objectives are the LCOE and the Renewable Energy Curtailment (REC). Optimization problems can be solved using either rule-based or optimization-based approaches. The former typically employs meta-heuristic methods, while the latter often relies on Mixed-Integer Linear Programming (MILP) models. This work adopts a rule-based approach using an in-house developed software that employs the Particle Swarm Optimization (PSO) algorithm.

The main goal of this paper is to investigate how the optimal sizing of a 100% RES system is affected when constraints on REC are imposed. Additionally, the study seeks to determine how a reduction of the storage technologies' cost could lead to a reduction of curtailment in the optimal configuration.

## 2 METHODOLOGY

A meta-heuristic optimization framework is implemented in Python to perform a multi-objective optimization using the ε-constraint method. The algorithm chosen is the adaptive PSO proposed by Zhan et al. (2009) and implemented through the Python library Pymoo (Blank and Deb, 2020). The following subsections describe the energy system modeling, the optimization approach, the economic parameters utilized, and the selected case study. The proposed layout of the 100% RES is shown in Figure 1, where electricity is generated by wind turbines and photovoltaic panels, and energy balance is maintained through a combination of BESS and HSS to ensure a continuous power supply that meets the island's electricity demand. The HSS includes an electrolyzer to produce hydrogen from renewable energy, a compressor to increase the hydrogen pressure to store it in a tank, and a fuel cell to reconvert hydrogen to electricity when needed. Different system configurations were analyzed, each incorporating different combinations of storage technologies (BESS, HSS, hybrid BESS+HSS) to assess the impact of hybridization on system performance.

### 2.1 Energy System Modelling and Management

The optimization considers a one-year time horizon with an hourly discretization timestep ($t$), and it is executed using an in-house developed Python-based software called Multi Energy System Simulator (MESS). MESS is a modular, rule-based model (Ademollo et al., 2025; Mati et al., 2023) that enables the optimal sizing of energy system components. Input data include electrical demand profile and meteorological conditions, such as solar irradiance and wind speed, as well as technical and economic parameters of system components. The key outputs of the optimization include the optimal sizing of the components, along with economic metrics such as the Levelized Cost of Electricity.

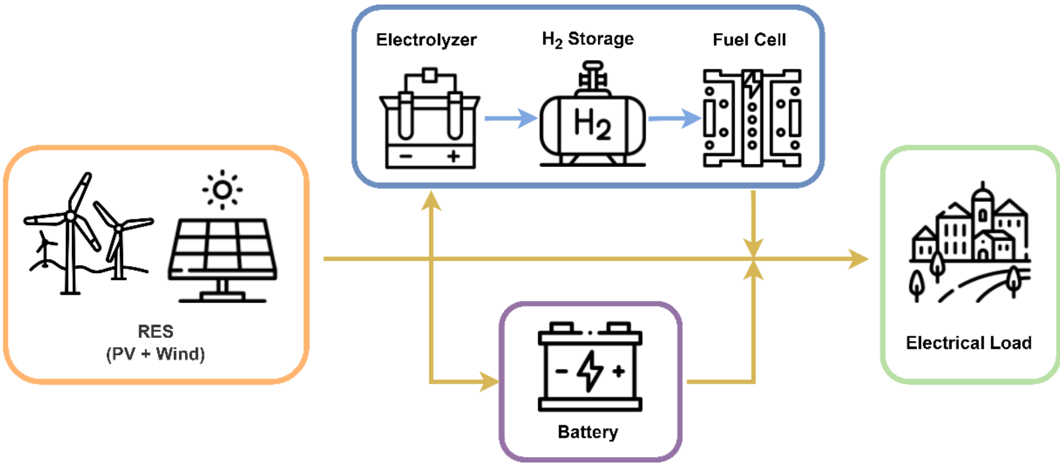


**Figure 1**: Layout of the renewable energy system.

Therefore, at each timestep, the system must satisfy the energy balance in Equation (1):

$$P_{\mathrm{PV}}(t) + P_{\mathrm{WT}}(t) + P_{\mathrm{FC}}(t) + P_{\mathrm{BT,dis}}(t) = P_{\mathrm{DEM}}(t) + P_{\mathrm{EL}}(t) + P_{\mathrm{CO}}(t) + P_{\mathrm{BT,ch}}(t) + P_{\mathrm{CURT}}(t) \quad (1)$$

Where $P_{\mathrm{PV}}(t)$ and $P_{\mathrm{WT}}(t)$ are the power generated respectively by the photovoltaic (PV) and wind turbine, $P_{\mathrm{BT,dis}}(t)$ and $P_{\mathrm{BT,ch}}(t)$ represent the battery's discharging and charging power, $P_{\mathrm{FC}}(t)$, $P_{\mathrm{EL}}(t)$ and $P_{\mathrm{CO}}(t)$ correspond to the operating power of the fuel cell, the electrolyzer, and the compressor, $P_{\mathrm{DEM}}(t)$ is the electricity demand of the system and $P_{\mathrm{CURT}}(t)$ is the power curtailment of VRES, all expressed in kW.

The system's energy management follows a rule-based algorithm implemented in MESS. At each timestep, the electricity demand and the renewable energy production are determined. When VRES production exceeds demand, the surplus is allocated to storage systems, with priority given to the battery. This prioritization is based on the battery's role as a short-term storage solution, while hydrogen storage is designed for seasonal balancing. If both storage systems reach full capacity, any additional renewable generation is curtailed. Conversely, when electricity demand exceeds renewable energy production, electricity load is met by discharging the battery first, followed by the fuel cell if additional energy is required.

The photovoltaic system's energy production was obtained from the Photovoltaic Geographical Information System (PVGIS) database (JRC, 2024), using location-specific hourly data. The selected configuration corresponds to a fixed system with tilt and azimuth angles optimized for the site, resulting in values of 32° and 7°, respectively. A system loss of 14%, as recommended by PVGIS, was applied. Consequently, the specific energy production at each timestep is determined, and the total power output of the PV system $P_{\mathrm{PV}}$ can be calculated by multiplying the specific production for the nominal power of the plant $P_{\mathrm{PV,r}}$.

The wind turbine's power output was estimated using a characteristic power curve, which expresses power as a function of wind speed, as described in Equation (2) (Deshmukh and Deshmukh, 2008). Wind speed data were retrieved from PVGIS at a reference height ($h_{\mathrm{ref}}$) of 10 m and were corrected to the turbine hub height ($h_{\mathrm{WT}}$) of 80 m using the power law shown in Equation (3). The power law exponent $\alpha$ was set to 0.17, based on the mean wind speed velocity at turbine height and at reference height, as reported by the Italian Wind Atlas (Sperati et al., 2024). In Equation (2), $v_{\mathrm{w,ci}}$, $v_{\mathrm{w,co}}$ and $v_{\mathrm{w,r}}$ are respectively the cut-in (3 m/s), cut-out (25 m/s) and rated wind speed (13 m/s), while $P_{\mathrm{WT,r}}$ is the rated power of the turbine, in kW. In Equation (3), $v_{\mathrm{w,ref}}$ is the wind speed measured at the reference height (in m/s).

$$P_{\mathrm{WT}}(t) = \begin{cases} 0, & v_{\mathrm{w}}(t) \le v_{\mathrm{w,ci}} \\ P_{\mathrm{WT,r}} \cdot \dfrac{v_{\mathrm{w}}^3(t) - v_{\mathrm{w,ci}}^3}{v_{\mathrm{w,r}}^3 - v_{\mathrm{w,ci}}^3}, & v_{\mathrm{w,ci}} \le v_{\mathrm{w}}(t) \le v_{\mathrm{w,r}} \\ P_{\mathrm{WT,r}}, & v_{\mathrm{w,r}} \le v_{\mathrm{w}}(t) \le v_{\mathrm{w,co}} \\ 0, & v_{\mathrm{w}}(t) \ge v_{\mathrm{w,co}} \end{cases} \tag{2}$$

$$v_{\mathrm{w}}(t) = v_{\mathrm{w,ref}}(t) \cdot \left(\frac{h_{\mathrm{WT}}}{h_{\mathrm{ref}}}\right)^{\alpha} \tag{3}$$

The energy stored in both storage systems is dynamically updated at each timestep. For the BESS, lithium-ion technology was selected due to its superior performance compared to lead-acid alternative. Charge and discharge efficiencies $\eta_{\mathrm{BT,ch}}$ and $\eta_{\mathrm{BT,dis}}$ were set at 95% (Moretti et al., 2019). The self-discharge rate $\sigma$ was defined to ensure a monthly self-discharge of 5% (Gracia et al., 2018). The State of Charge ($SOC$), defined as the ratio of stored energy to the nominal battery capacity $Cap_{\mathrm{BT}}$, is constrained within a minimum ($SOC_{\mathrm{min}}$) and a maximum limit ($SOC_{\mathrm{max}}$) to ensure operational safety. While $SOC_{\mathrm{max}}$ has been set to 1, a $SOC_{\mathrm{min}}$ threshold of 20% is always maintained to prevent deep discharge and ensure battery longevity (Gracia et al., 2018). Equations (4) and (5) resume the SOC's dynamic update:

$$SOC(t+1) = SOC(t) \cdot (1-\sigma) + \frac{P_{\mathrm{BT,ch}}(t) \cdot \Delta t \cdot \eta_{\mathrm{BT,ch}}}{Cap_{\mathrm{BT}}} - \frac{P_{\mathrm{BT,dis}}(t) \cdot \Delta t}{Cap_{\mathrm{BT}} \cdot \eta_{\mathrm{BT,dis}}} \tag{4}$$

$$SOC_{\mathrm{min}} \le SOC(t) \le SOC_{\mathrm{max}} \tag{5}$$

The Hydrogen Storage System employs Proton-Exchange Membrane (PEM) technology for both the electrolyzer and fuel cell, as it provides a rapid response to fluctuating renewable energy inputs (Nikolaidis and Poullikkas, 2017). A detailed model of the PEM electrolyzer and fuel cell has been implemented in MESS following Lubello et al. (2022). The electrolyzer operates up to 30 bar with a nominal efficiency of 66.0% equivalent to a conversion efficiency of 50.5 kWh/$kg_{H2}$. The fuel cell operates at ambient pressure with a nominal efficiency of 42.8% corresponding to a conversion efficiency of 0.070 $kg_{H2}$/kWh, based on hydrogen's Lower Heating Value (LHV). The conversion efficiencies determine the hydrogen mass flow rates for both production ($m_{\mathrm{H2,EL}}$) and consumption ($m_{\mathrm{H2,FC}}$). To prevent membrane degradation at low partial loads, a minimum operating power of 10% is imposed for both the electrolyzer and the fuel cell. Each system consists of 100 kW modules operating in parallel. If the available power is insufficient to sustain at least 10% capacity per module, the system dynamically adjusts the number of active modules to ensure stable operation. The Level of Hydrogen (LOH) in the storage tank, defined as the ratio of the stored hydrogen to the total tank capacity, is updated dynamically at each timestep, balancing hydrogen production and demand, as shown in Equation (6):

$$LOH(t+1) = LOH(t) + \frac{m_{\mathrm{H2,EL}}(t)}{Size_{\mathrm{HT}}} - \frac{m_{\mathrm{H2,FC}}(t)}{Size_{\mathrm{HT}}} \tag{6}$$

The water consumption $cons_{\mathrm{H2O,EL}}$ (in $m^3$) for the operation of the electrolyzer is calculated by multiplying the hydrogen production by a water consumption factor, equal to 15 $m^3_{H20}$/$kg_{H2}$ (Singlitico et al., 2021). The storage system consists of a seamless steel tank pressurized at 200 bar. Hydrogen from the electrolyzer is compressed from 30 to 200 bar using a centrifugal compression system, with a specific energy consumption of 1.76 kWh/$kg_{H2}$ (Tractebel et al., 2017).

## 2.2 Sizing approach

The system sizing was performed using the Particle Swarm Optimization algorithm to optimize component sizes while minimizing both the LCOE and the REC. The multi-objective optimization was conducted using the ε-constraint method. First, a single-objective optimization minimizes the LCOE without any constraint on the curtailment. The formula for estimating the LCOE (in €/kWh) is presented in Equation (7):

$$LCOE = \frac{\sum_k C_{\mathrm{inv},k} * (1 + c_{\mathrm{eng}} + c_{\mathrm{inst}}) \; + \sum_{j=1}^{n} \frac{\left(\sum_k C_{\mathrm{rep},k,j} + C_{\mathrm{O\&M},j}\right)}{(1+d)^j}}{\sum_{j=1}^{n} \frac{E_{tot,j}}{(1+d)^j}} \tag{7}$$

Where $E_{tot,j}$ (in kWh) is the total electricity demand met in the j-th year, $C_{\mathrm{inv},k}$ (in €) is the investment cost of the k-th component, with additional engineering ($c_{\mathrm{eng}}$) and installation ($c_{\mathrm{inst}}$) costs as a percentage of the investment, $C_{\mathrm{rep},k,j}$ represents the replacement cost (in €) of the k-th component during the j-th year, determined by multiplying the component investment cost by a replacement rate. The term $C_{\mathrm{O\&M},j}$ is the annual Operating Expenditures (OPEX) for the j-th year that includes the maintenance costs for all components and the water cost for the PEM electrolyzer. Finally, $n$ is the lifetime of the project, set at 20 years, while $d$ is the real discount rate, which accounts for the nominal discount rate ($d'$) and the inflation rate ($ir$) using Fisher's equation, as displayed in Equation (8). The nominal discount rate was set at 7%, while the inflation rate chosen is the average in the Euro Area in the last 30 years, equal to 2.23% (Trading Economics, 2024).

$$d = \frac{1 + d'}{1 + ir} - 1 \tag{8}$$

Economic data used for the analysis are detailed in Table 1 and Table 2. Component costs are derived from authoritative sources, including the International Energy Agency (IEA-Wind, 2023; IEA-PVPS, 2022), the Danish Energy Agency (DEA, 2024a.; DEA, 2024b; DEA, 2024c), and the National Renewable Energy Laboratory (NREL, 2024a; NREL, 2024b; NREL, 2024c).

**Table 1*:*** Economic parameters for components.

| **Component** | **CAPEX** | **OPEX** | **Lifetime** | **Replacement** |
|---|---|---|---|---|
| PV | 1060 €/kW | 2% $C_{\mathrm{inv,PV}}$ | Project | - |
| Wind | 1200 €/kW | 3% $C_{\mathrm{inv,wind}}$ | Project | - |
| BESS | 450 €/kWh | 2.5% $C_{\mathrm{inv,BT}}$ | 15 | 50% $C_{\mathrm{inv,BT}}$ |
| Electrolyzer | 1196 €/kW | 5% $C_{\mathrm{inv,EL}}$ | 10 | 50% $C_{\mathrm{inv,EL}}$ |
| Fuel Cell | 1300 €/kW | 5% $C_{\mathrm{inv,FC}}$ | 10 | 20% $C_{\mathrm{inv,FC}}$ |
| $H_2$ Tank | 230 €/kg | 2% $C_{\mathrm{inv,HT}}$ | Project | - |
| Compressor | 4577 €/kW | 4% $C_{\mathrm{inv,CO}}$ | Project | - |

**Table 2:** Energy costs and financial parameters.

| **Energy Costs** | **Value** |
|---|---|
| Demineralized Water | 4 €/m$^3$ |
| **Financial Parameters** | **Value** |
| Nominal discount rate | 7% |
| Inflation rate | 2.23% |
| Cost of engineering | 15% $C_{\mathrm{inv}}$ |
| Cost of installation | 15% $C_{\mathrm{inv}}$ |
| Project Lifetime | 20 years |

The renewable energy curtailment in the cost-optimized scenario $E_{\mathrm{CURT,max}}$ (in kWh) is given by Equation (9):

$$E_{\text{CURT,max}} = \sum\nolimits_{t=t_{start}}^{t_{end}} P_{\text{CURT}}(t) \cdot \Delta\text{t} \tag{9}$$

The range of curtailment values – from maximum curtailment to zero curtailment – was divided into n steps. The Pareto front was then constructed by solving n single-objective problems, each minimizing LCOE while satisfying a constraint on the corresponding annual curtailment $E_{\text{CURT,target}}$.

### 2.3 Pantelleria case study

The island of Pantelleria in Italy was selected as a case study due to its geographical position and characteristics. Its significant distance from the mainland makes a connection to the national electricity grid unfeasible. Electricity demand is primarily met by diesel generators, with only 1 MW of installed PV capacity as of 2020 (European Commission, 2020), which results in high annual costs and $CO_2$ emissions. Despite this, Pantelleria has significant renewable energy potential. An analysis based on the PVGIS Typical Meteorological Year (TMY) dataset indicates an energy yield of 1641.9 kWh/kW$_p$ from PV, corresponding to a capacity factor of 18.74%. Wind energy potential is even higher, with an estimated yield of 3298.0 kWh/kW$_p$, and a corresponding capacity factor of 37.65%. To model electricity consumption, real monthly data were retrieved from the "Clean Energy for EU Island" report (European Commission, 2020). To obtain an hourly demand profile, the Italian agency for Energy System Research (RSE) tool "TOTEM" was used (RSE, 2021). The island's electricity consumption closely follows seasonal tourism patterns, peaking during the summer months. The total annual electricity demand amounts to 31.1 GWh. Figure 2 presents a summary of the island's renewable energy potential and the hourly electricity load profile over a year.

## 3 RESULTS

The Pareto cost-curtailment fronts were generated for the three storage configurations (BESS, HSS, BESS+HSS) starting from an economic optimization unconstrained on the amount of curtailment. Subsequent front points were obtained by reducing the initial curtailment level in six successive steps (-20%, -40%, -60%, -80%, -90%, -100%). The results, illustrated in Figure 3, demonstrate that a reduction in RES curtailment is accompanied by an increase in LCOE for each storage scenario. However, the magnitude of this growth varies significantly. It is evident that the BESS scenario is unsuitable for a fully renewable system. Among the three configurations, BESS consistently results in the highest LCOE, but the gap widens when the constraint is stricter, leading to an exorbitant LCOE of 5.157 €/kWh when curtailment is eliminated, compared with 0.513 €/kWh for the HSS and 0.388 €/kWh for the hybrid configuration. The minimum LCOE for BESS is 0.315 €/kWh and occurs with a curtailment of 30.4 GWh (48.5% of VRES production). By comparison, the HSS achieves a lower LCOE of 0.295 €/kWh with 26.6 GWh of curtailment (37.6% of production), and the hybrid system outperforms both, yielding a minimum LCOE of 0.287 €/kWh with 25.5 GWh of curtailment (40.7% of production).

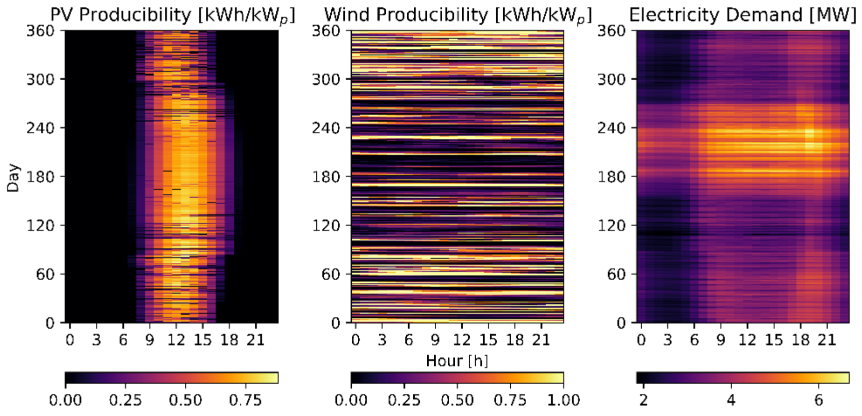


**Figure 2**: Heatmaps of PV, Wind producibility, and Electricity demand over a year.

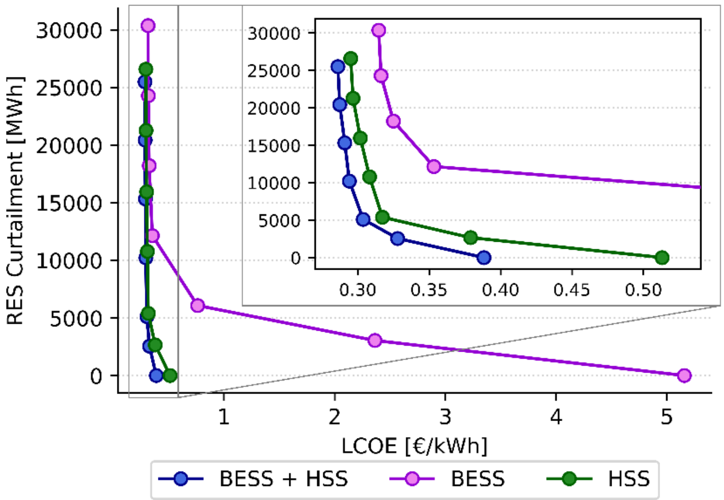


**Figure 3**: Cost-Curtailment Pareto Fronts in BESS, HSS, and BESS+HSS configurations.

The analysis of Figure 3 highlights the advantages of hybrid storage in balancing cost efficiency with curtailment reduction. The hybrid configuration enables a trade-off between these two objectives. For instance, a 60% reduction in curtailment leads to an LCOE of 0.294 €/kWh, only 2.4% higher than the optimal one achieved without curtailment constraints.

An investigation of the variations in component sizes from the economic optimal solution to the one with zero curtailment is presented in Figure 4, revealing expected trends. Across all configurations, reducing curtailment is associated with a decrease in the power generation capacity and an increase in storage systems size. This effect is particularly pronounced in battery-based systems. Given the BESS's inadequacy to provide seasonal storage, the economically optimal solution requires substantial PV oversizing (35.20 MW) and a relatively small battery capacity (74.70 MWh). Conversely, when a zero-curtailment constraint is imposed, the PV capacity is significantly reduced (15.52 MW) while the battery storage is drastically increased to 2460 MWh. It is noteworthy that wind turbines have low sizes in the BESS scenario (from 1.47 MW to 2.40 MW). This is due to the seasonal nature of wind generation, which peaks in winter when electricity demand is relatively low. Consequently, wind power becomes less suitable in a scenario where the storage system has a duration of only a few hours. The other two scenarios achieve a more balanced distribution of renewable energy sources, with a corresponding decrease in size in both cases, as delineated in Table 3. Consequently, there is an increase in the hydrogen storage tank from 89.72 to 162.00 tons in the HSS case and from 64.08 to 122.03 tons in the hybrid case. Notably, in the hybrid scenario, battery capacity remains relatively stable across different curtailment levels, suggesting that the system effectively utilizes hydrogen storage to compensate for seasonal imbalances. The increase in tank dimensions is concomitant with an increase in the sizes of the electrolyzer and the fuel cell, as delineated in Table 3.

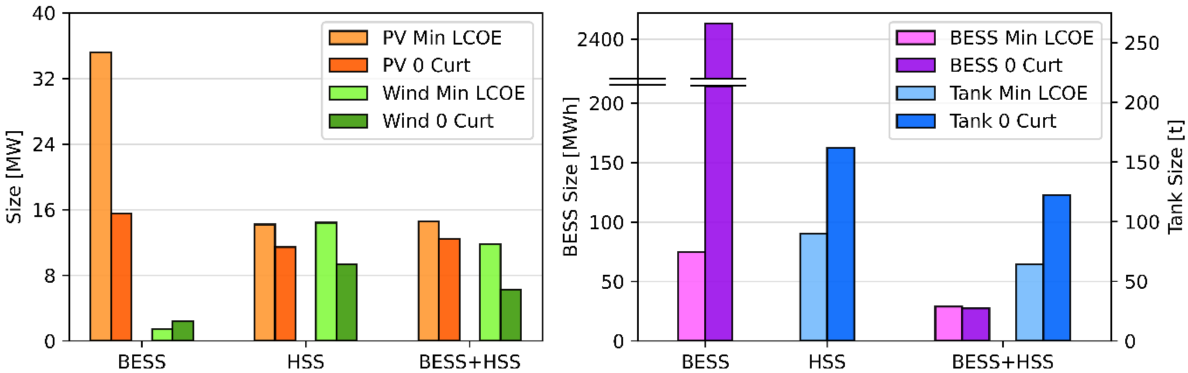


**Figure 4**: Component Sizes for minimum LCOE and zero curtailment in the different configurations.

**Table 3**: Component Sizes for minimum LCOE and zero curtailment in the different configurations.

| Component | BESS | | HSS | | BESS+HSS | |
|---|---|---|---|---|---|---|
| | **Min LCOE** | **0 Curt** | **Min LCOE** | **0 Curt** | **Min LCOE** | **0 Curt** |
| PV [MW] | 35.20 | 15.52 | 14.20 | 11.43 | 14.55 | 12.44 |
| Wind [MW] | 1.47 | 2.40 | 14.40 | 9.36 | 11.77 | 6.23 |
| BESS [MWh] | 74.70 | 2459.99 | - | - | 28.74 | 27.32 |
| Electrolyzer [MW] | - | - | 3.80 | 17.40 | 2.00 | 12.00 |
| Fuel Cell [MW] | - | - | 4.20 | 13.80 | 3.00 | 3.40 |
| $H_2$ Tank [t] | - | - | 89.72 | 162.00 | 64.08 | 122.03 |

The different operational characteristics of the storage systems are reflected in their level of charge trends, as depicted in Figure 5. The hydrogen tank, represented on the right, exhibits a seasonal storage pattern across all scenarios, with variations depending on the specific configuration. Conversely, the battery displays a seasonal trend exclusively in the BESS configuration with zero curtailment. In the other scenarios, the battery's size is considerably smaller, and its state of charge undergoes more frequent charging and discharging cycles, aligning with the short-term energy balancing role it plays.
These differences translate directly into the system's economic performance. Figure 6 illustrates the contribution of the various technologies to the LCOE under different curtailment levels. Across all the scenarios, as the system transitions from the minimum LCOE to a zero-curtailment solution, the cost contribution of renewable energy generation decreases, while the share of storage-related costs increases. This shift is most pronounced in the BESS scenario, where the need for very high battery capacity drives up costs. In contrast, in the hybrid configuration, the presence of a battery as a short-term storage solution reduces the required size of hydrogen storage components, particularly the fuel cell, leading to a more cost-effective system compared to the HSS-only scenario.
In conclusion, a sensitivity analysis was conducted on the hybrid configuration to evaluate whether a reduction in storage system prices could render curtailment minimization economically beneficial. The analysis considered simultaneous reductions in battery, electrolyzer, fuel cell and hydrogen tank costs. The results, illustrated in Figure 7 indicate that cost reductions lead to a notable decrease in curtailment levels of the optimal system configuration. Specifically, with an 80% reduction in storage costs, curtailment decreases from 24.6 GWh to 4.0 GWh, while the disparity in LCOE between the optimal and zero-curtailment scenarios narrows from 0.101 €/kWh to just 0.016 €/kWh. While future price trends remain uncertain, estimates (Cole and Karmakar, 2023; IRENA, 2020) indicate a reduction in utility-scale battery costs of 30% by 2030 and of 55% by 2050, while electrolyzer costs are expected to decline by 60% by 2030 and between 80 and 88% by 2050, depending on the installed capacity. These projections suggest that a zero-curtailment solution could become the economically optimal choice in the future, provided that widespread deployment of storage and conversion technologies drives the anticipated cost reductions.

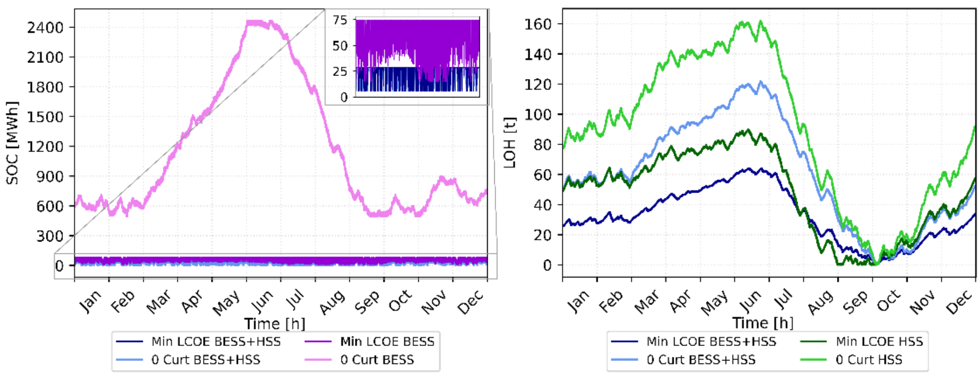


**Figure 5**: Battery SOC (left) and Hydrogen LOH (right) in the different scenarios.

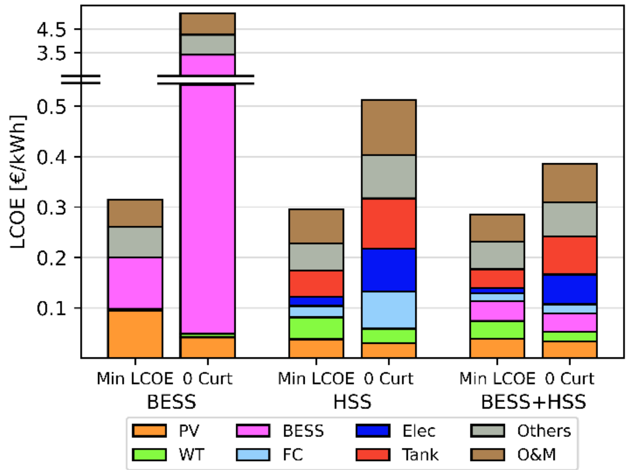


**Figure 6**: Components' contribution to the LCOE in the different configurations.

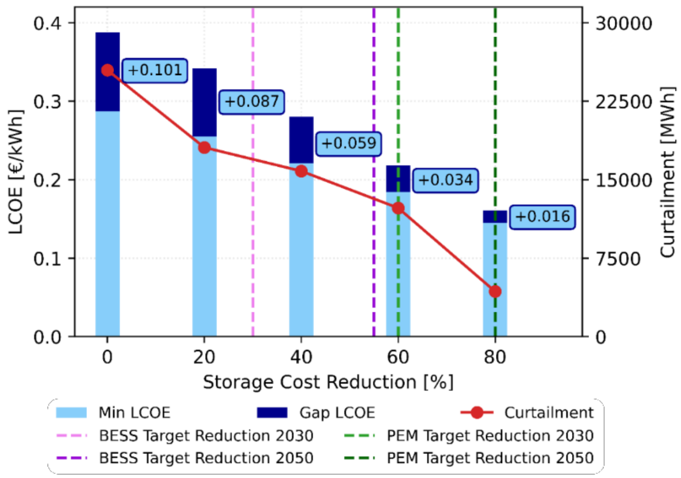


**Figure 7**: Price Gap between optimal and zero curtailment solutions at different storage prices.

## 4 CONCLUSIONS

This study presents a multi-objective optimization of an isolated fully renewable system, evaluating different storage configurations and their impact on LCOE and renewable energy curtailment. The key findings can be summarized as follows:

- The use of batteries alone is not adequate for a fully renewable stand-alone energy system, especially when curtailment reduction is a priority. The BESS-only configuration results in significantly higher LCOE, particularly under strict curtailment constraints.
- Hybrid storage, integrating both BESS and HSS, provides the best economic performance across all the levels of curtailment. It achieves the lowest LCOE of 0.287 €/kWh and maintains a relatively modest increase at zero curtailment (0.388 €/kWh), demonstrating the advantages of storage hybridization.
- A 60% reduction in curtailment in the hybrid storage configuration results in only a marginal 2.4% increase in LCOE, indicating that curtailment minimization can be achieved without excessive economic penalties when storage is properly integrated.
- Across all configurations, reducing curtailment necessitates an increase in storage system size while allowing for a reduction in power generation capacity. This trend is particularly evident in battery-based systems, where curtailment elimination requires substantial battery oversizing.

- Sensitivity analysis indicates that a reduction in storage and conversion technologies price could enhance the economic feasibility of curtailment minimization. A projected 80% reduction in storage costs could reduce curtailment from 24.6 GWh to 4.0 GWh, while narrowing the LCOE gap between optimal and zero-curtailment solutions from 0.101 €/kWh to just 0.016 €/kWh.

Overall, the study highlights that hybrid storage solutions offer the most effective trade-off between cost and curtailment reduction in isolated fully renewable energy systems. Future developments in storage technologies could further enhance the viability of achieving zero curtailment solutions. Further research could explore advanced energy management strategies and the integration of demand-side flexibility to improve the overall efficiency of the system.

## NOMENCLATURE

| | | |
|---|---|---|
| BESS | Battery Electricity Storage System | |
| $c$ | Specific cost | (€/kWh) |
| $C$ | Cost | (€) |
| $Cap$ | Capacity | (kWh) |
| $cons$ | Consumption | ($m^3$) |
| $d$ | Real discount rate | (-) |
| $d'$ | Nominal discount rate | (-) |
| DG | Diesel Generator | |
| $E$ | Energy | (kWh) |
| ESS | Energy Storage System | |
| $h$ | Height | (m) |
| HSS | Hydrogen Storage System | |
| $ir$ | Inflation rate | (-) |
| $LCOE$ | Levelized Cost of Electricity | (€/kWh) |
| LHV | Lower Heating Value | (kWh/kg) |
| $LOH$ | Level of Hydrogen | (-) |
| $m$ | Mass flow rate | (kg/s) |
| MESS | Multi Energy System Simulator | |
| MILP | Mixed Integer Linear Programming | |
| $n$ | Lifetime | (years) |
| OPEX | Operational Expenditures | |
| $P$ | Power | (kW) |
| PEM | Proton-Exchange Membrane | |
| PSO | Particle Swarm Optimization | |
| PVGIS | Photovoltaic Geographical Information System | |
| REC | Renewable Energy Curtailment | |
| RES | Renewable Energy System | |
| RSE | Italian agency for energy system research | |
| $Size$ | Size | (kg) |
| $SOC$ | State of Charge | (-) |
| $t$ | Timestep | (h) |
| TMY | Typical Meteorological Year | |
| v | Velocity | (m/s) |
| VRES | Variable Renewable Energy Source | |
| $\alpha$ | Power law exponent | (-) |
| $\eta$ | Efficiency | (%) |
| $\sigma$ | Self-discharge rate | ($h^{-1}$) |

**Subscript**

| | | | |
|---|---|---|---|
| BT | Battery | co | Cut-out |
| ci | Cut-in | CO | Compressor |
| ch | Charge | CURT | Curtailment |

| | | | |
|---|---|---|---|
| DEM | Demand | max | Maximum |
| dis | Discharge | O&M | Operation and Maintainance |
| EL | Electrolyzer | PV | Photovoltaic |
| end | End | r | Rated |
| eng | Engineering | ref | Reference |
| FC | Fuel Cell | rep | Replacement |
| H2 | Hydrogen | start | Start |
| H2O | Water | target | Target |
| HT | Hydrogen Tank | tot | Total |
| inst | Installation | w | Wind speed |
| inv | Investment | WT | Wind Turbine |
| min | Minimum | | |

## REFERENCES

Ademollo, A., Calabrese, M., Carcasci, C., 2025. An up-to-date perspective of levelized cost of hydrogen for PV-based grid-connected power-to-hydrogen plants across all Italy. Appl Energy 379, 124958. https://doi.org/10.1016/J.APENERGY.2024.124958

Blank, J., Deb, K., 2020. Pymoo: Multi-Objective Optimization in Python. IEEE Access 8, 89497–89509. https://doi.org/10.1109/ACCESS.2020.2990567

Borhanazad, H., Mekhilef, S., Gounder Ganapathy, V., Modiri-Delshad, M., Mirtaheri, A., 2014. Optimization of micro-grid system using MOPSO. Renew Energy 71, 295–306. https://doi.org/10.1016/J.RENENE.2014.05.006

Brinkhaus, M., Jarosch, D., Kapischke, J., 2011. All year power supply with off-grid photovoltaic system and clean seasonal power storage. Solar Energy 85, 2488–2496. https://doi.org/10.1016/J.SOLENER.2011.07.007

Cole, W., Karmakar, A., 2023. Cost Projections for Utility-Scale Battery Storage: 2023 Update. https://doi.org/10.2172/1984976

Danish Energy Agency, 2024a. Technology Data for Energy Storage. URL https://ens.dk/en/analyses-and-statistics/technology-data-energy-storage (accessed 1.31.25).

Danish Energy Agency, 2024b. Technology Data for Generation of Electricity and District Heating URL https://ens.dk/en/analyses-and-statistics/technology-data-generation-electricity-and-district-heating (accessed 1.31.25).

Danish Energy Agency, 2024c. Technology Data for Renewable Fuels URL https://ens.dk/en/analyses-and-statistics/technology-data-renewable-fuels (accessed 1.31.25).

Deshmukh, M.K., Deshmukh, S.S., 2008. Modeling of hybrid renewable energy systems. Renewable and Sustainable Energy Reviews 12, 235–249. https://doi.org/10.1016/J.RSER.2006.07.011

European Commission, 2020. Pantelleria | Clean energy for EU islands. URL https://clean-energy-islands.ec.europa.eu/countries/italy/pantelleria (accessed 1.31.25).

Gracia, L., Casero, P., Bourasseau, C., Chabert, A., 2018. Use of Hydrogen in Off-Grid Locations, a Techno-Economic Assessment. Energies 2018, Vol. 11, Page 3141 11, 3141. https://doi.org/10.3390/EN11113141

IEA, 2024 Islands need resilient power systems more than ever. Clean energy can deliver – Analysis – IEA. URL https://www.iea.org/commentaries/islands-need-resilient-power-systems-more-than-ever-clean-energy-can-deliver (accessed 1.31.25).

IEA-PVPS, 2022. National Survey Reports Archive – Italy URL https://iea-pvps.org/national-survey-reports/?year_p=116&country=&order=DESC&keyword= (accessed 1.31.25).

IEA Wind, 2023. Report 2023, Italy. URL https://iea-wind.org/ (accessed 1.31.25).

IRENA, 2020. Green Hydrogen Cost Reduction: Scaling up Electrolysers to Meet the 1.5$^0$C Climate Goal. International Renewable Energy Agency 105. URL https://www.irena.org/publications/2020/Dec/Green-hydrogen-cost-reduction (accessed 1.31.25)

JRC, 2024. Photovoltaic Geographical Information System (PVGIS) - European Commission URL https://re.jrc.ec.europa.eu/pvg_tools/en/ (accessed 1.31.25).

Lubello, P., Pasqui, M., Mati, A., Carcasci, C., 2022. Assessment of hydrogen-based long term electrical energy storage in residential energy systems. Smart Energy 8, 100088. https://doi.org/10.1016/J.SEGY.2022.100088
Mahbub, M.S., Viesi, D., Cattani, S., Crema, L., 2017. An innovative multi-objective optimization approach for long-term energy planning. Appl Energy 208, 1487–1504. https://doi.org/10.1016/J.APENERGY.2017.08.245
Mahbub, M.S., Viesi, D., Crema, L., 2016. Designing optimized energy scenarios for an Italian Alpine valley: the case of Giudicarie Esteriori. Energy 116, 236–249. https://doi.org/10.1016/J.ENERGY.2016.09.090
Marocco, P., Ferrero, D., Lanzini, A., Santarelli, M., 2022. The role of hydrogen in the optimal design of off-grid hybrid renewable energy systems. J Energy Storage 46, 103893. https://doi.org/10.1016/J.EST.2021.103893
Mati, A., Ademollo, A., Carcasci, C., 2023. Assessment of paper industry decarbonization potential via hydrogen in a multi-energy system scenario: A case study. Smart Energy 11, 100114. https://doi.org/10.1016/J.SEGY.2023.100114
Meschede, H., Bertheau, P., Khalili, S., Breyer, C., 2022. A review of 100% renewable energy scenarios on islands. Wiley Interdiscip Rev Energy Environ 11, e450. https://doi.org/10.1002/WENE.450
Moretti, L., Astolfi, M., Vergara, C., Macchi, E., Pérez-Arriaga, J.I., Manzolini, G., 2019. A design and dispatch optimization algorithm based on mixed integer linear programming for rural electrification. Appl Energy 233–234, 1104–1121. https://doi.org/10.1016/J.APENERGY.2018.09.194
Nikolaidis, P., Poullikkas, A., 2017. A comparative overview of hydrogen production processes. Renewable and Sustainable Energy Reviews 67, 597–611. https://doi.org/10.1016/J.RSER.2016.09.044
NREL, 2024a. Land-Based Wind | Electricity | 2024 | ATB | NREL URL https://atb.nrel.gov/electricity/2024/land-based_wind (accessed 1.31.25).
NREL, 2024b. Utility-Scale Battery Storage | Electricity | 2024 | ATB | NREL. URL https://atb.nrel.gov/electricity/2024/utility-scale_battery_storage (accessed 1.31.25).
NREL, 2024c. Utility-Scale PV | Electricity | 2024 | ATB | NREL. URL https://atb.nrel.gov/electricity/2024/utility-scale_pv (accessed 1.31.25).
RSE, 2021. TOTEM. URL https://totem.rse-web.it/ (accessed 1.31.25).
Singlitico, A., Østergaard, J., Chatzivasileiadis, S., 2021. Onshore, offshore or in-turbine electrolysis? Techno-economic overview of alternative integration designs for green hydrogen production into Offshore Wind Power Hubs. Renewable and Sustainable Energy Transition 1, 100005. https://doi.org/10.1016/J.RSET.2021.100005
Song, J., Oh, S.D., Yoo, Y., Seo, S.H., Paek, I., Song, Y., Song, S.J., 2018. System design and policy suggestion for reducing electricity curtailment in renewable power systems for remote islands. Appl Energy 225, 195–208. https://doi.org/10.1016/J.APENERGY.2018.04.131
Sperati, S., Alessandrini, S., D'Amico, F., Cheng, W., Rozoff, C.M., Bonanno, R., Lacavalla, M., Aiello, M., Airoldi, D., Amaranto, A., Decimi, G., Vergata, M.A., 2024. A new Wind Atlas to support the expansion of the Italian wind power fleet. Wind Energy 27, 298–316. https://doi.org/10.1002/WE.2890
Tractebel, Engie, Hinicio, 2017. Study on Early Business Cases for H2 in Energy Storage and More Broadly Power to H2 Applications.
Trading Economics, 2024. Euro Area Inflation Rate. URL https://tradingeconomics.com/euro-area/inflation-cpi (accessed 1.31.25).
Wang, B., Zhou, M., Xin, B., Zhao, X., Watada, J., 2019. Analysis of operation cost and wind curtailment using multi-objective unit commitment with battery energy storage. Energy 178, 101–114. https://doi.org/10.1016/J.ENERGY.2019.04.108
Zhan, Z.H., Zhang, J., Li, Y., Chung, H.S.H., 2009. Adaptive particle swarm optimization. IEEE Transactions on Systems, Man, and Cybernetics, Part B: Cybernetics 39, 1362–1381. https://doi.org/10.1109/TSMCB.2009.2015956